

Efficient mode transformations of degenerate Laguerre–Gaussian beams

Galina Machavariani, Amiel A. Ishaaya, Liran Shimshi, Nir Davidson, Asher A. Friesem, and Erez Hasman

We present an approach for efficient conversion of a single-high-order-mode distribution from a laser to a nearly Gaussian distribution and vice versa. It is based on dividing the high-order mode distribution into equal parts that are then combined together coherently. We implement our approach with several optical arrangements that include a combination of discrete elements and some with single interferometric elements. These arrangements are analyzed and experimentally evaluated for converting the TEM_{01} mode distribution with $M_x^2 = 3$ to a nearly Gaussian beam with $M_x^2 = 1.045$ or $M_x^2 = 1.15$. The basic principle, design, and experimental results obtained with several conversion arrangements are presented. The results reveal that conversion efficiency is typically greater than 90%, compared with theoretical ones. In addition, some arrangement is exploited for converting the fundamental Gaussian-beam distribution into the TEM_{01} mode distribution. © 2004 Optical Society of America

OCIS code: 140.3300.

1. Introduction

The important properties of divergence and focusability for the beams that emerge from a laser depend mainly on their transverse intensity and phase distributions. Thus it is important to control such distributions. Indeed recent years have witnessed a growing interest in the formation of laser beams with specific intensity and phase distributions.^{1–8} Such specific distributions can be efficiently obtained either by introducing special elements into the cavity of the laser^{1–4} or by externally converting a given laser-beam distribution into the desired one.^{5–9} In principle, any laser beam with well-defined amplitude and phase distributions can be transformed to a desired well-defined beam by means of two specially designed external phase elements.^{8,9} Unfortunately the design and fabrication of such elements is usually difficult, if at all practical.

A related problem is how to efficiently convert a high-order transverse-mode TEM_{p1} distribution with poor beam quality but relatively high power^{1,2} to a Gaussian TEM_{00} distribution that has optimal beam quality ($M^2 = 1$). Recently we proposed a relatively simple method for such efficient conversion.¹⁰ It is based on the fact that the field distribution of high-order modes often consists of several bright spots (lobes), each of which has an intensity distribution that is rather close to that of the Gaussian beam. For example, the intensity distribution of each of the two lobes of the TEM_{01} mode has $M_x^2 = 1.15$, being very close to that of the Gaussian beam and much smaller than that of the whole TEM_{01} mode ($M_x^2 = 3$). Thus the high-order mode distribution can be divided into equal individual lobes that are then combined coherently.

In this paper we present a comprehensive theoretical and experimental investigation of the basics of our approach and present several conversion arrangements for implementing it. They include some with separate and discrete elements and some more compact and robust, with single interferometric elements. We discuss the advantages and disadvantages of each of these arrangements and present both analytical and experimental results. Also, we show that the arrangements can be exploited for efficiently converting a Gaussian-beam distribution to that of the TEM_{01} mode distribution.

G. Machavariani, A. A. Ishaaya, L. Shimshi, N. Davidson, and A. A. Friesem are with the Department of Physics of Complex Systems, Weizmann Institute of Science, Rehovot 76100, Israel (e-mail for G. Machavariani, galina@wisemail.weizmann.ac.il). E. Hasman is with the Optical Engineering Laboratory, Faculty of Mechanical Engineering, Technion—Israel Institute of Technology, Haifa 32000, Israel.

Received 2 October 2003; revised manuscript received 30 December 2003; accepted 30 January 2004.

0003-6935/04/122561-07\$15.00/0

© 2004 Optical Society of America

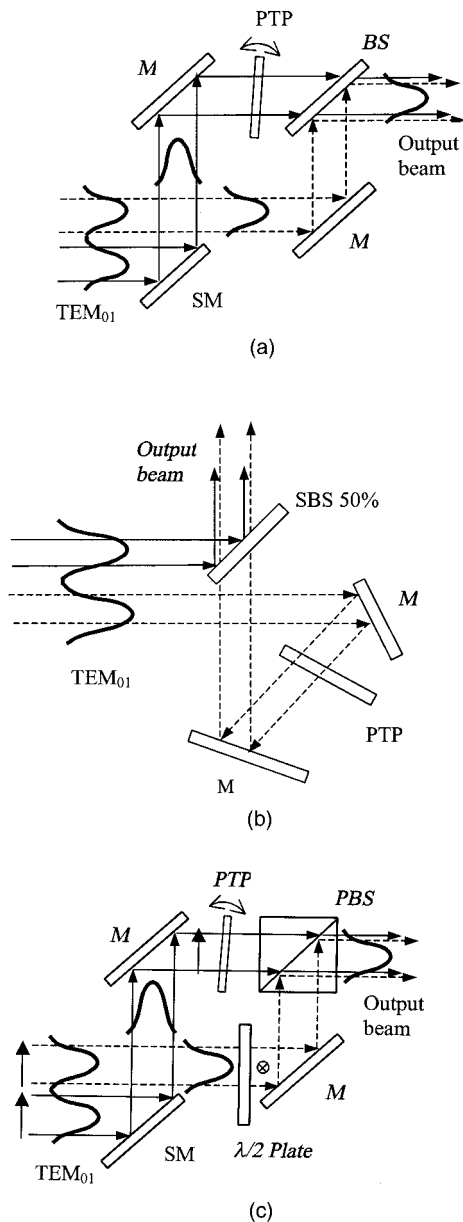


Fig. 1. Arrangements for converting a TEM_{01} mode distribution to nearly Gaussian distributions: (a) modified Mach-Zehnder interferometer arrangement with nonsymmetrical folding; (b) arrangement for symmetrical folding that allows exact matching of the individual lobes; (c) arrangement for nonsymmetrical folding that includes orthogonal polarizations.

2. Arrangements for Converting High-Order Mode Distributions into a Gaussian Distribution

Some possible arrangements, which include several discrete elements, for separating the TEM_{01} beam into two symmetric lobes and then combining them coherently are schematically shown in Fig. 1. Figure 1(a) shows a modified Mach-Zehnder interferometer. Here the sharp edge of a mirror, SM, is carefully aligned along the symmetry axis between the two lobes so as to reflect only one of them. Then the two beams are reflected by mirrors, M, and combined with a 50% beam splitter, BS. A phase tuning

plate, PTP, is inserted in the path of one of the beams in order to adjust the relative phase between them by the slight tilting of the plate. With appropriate phase adjustment the resulting combined output beam will emerge either to the right of the beam splitter or the directed upward. In the arrangement of Fig. 1(a) the field distribution of one lobe of the TEM_{01} mode distribution is shifted with respect to the other, yielding nonsymmetrical folding, whereby the two separated distributions cannot completely coincide. Thus there will be some power leakage. It is possible to prevent power leakage and obtain 100% conversion efficiency by adding or removing one reflection from one arm of the interferometer, as shown in Fig. 1(b). This enables exact matching between the two lobe distributions (as is evident from the inversion symmetry of the TEM_{01} mode distribution). In this case we obtain symmetrical folding, whereby the field distributions of the two lobes can be matched exactly. As discussed below, this modification should completely eliminate power leakage, however, causing slight degradation in the beam quality of the output beam.

Figure 1(c) shows another arrangement for nonsymmetrical folding that also involves orthogonal polarizations. In this arrangement a $\lambda/2$ plate is added to one arm of the interferometer, so the output is a combination of two orthogonally polarized lobes by the polarizing beam splitter, PBS. The advantages of this arrangement over that of previous arrangements are reduced alignment sensitivity and little if any power leakage. On the other hand, the polarization state of the output beam depends on the phase difference between the two combined lobes and is difficult to define.

The arrangements shown in Fig. 1 include several discrete optical elements that must be accurately aligned with respect to one another and must retain accurate interferometric stability. More robust, stable, and compact arrangements are presented in Fig. 2. Figure 2(a) shows a single interferometric element that performs both the needed separation of the two TEM_{01} lobes and their coherent summation. The interferometric element is a high-precision parallel plate with specially designed coatings, aligned at 45° angle to the collimated input beam of TEM_{01} distribution. One half of the front surface of the plate is coated with antireflection (AR) coating, while the other half with 50% reflection coating, so as to serve as the beam splitter, BS. The back surface is coated with a highly reflective coating. The plate is carefully aligned so that the border between the two front coatings separates the two lobes symmetrically. One of the lobes is transmitted through the AR coating region and reflected from the rear surface, where it coherently superimposes on the other lobe at the BS surface. As in the arrangement in Fig. 1(a), one lobe is effectively shifted with respect to the other and not flipped, so the field distributions of the two lobes do not exactly coincide. For the two lobes to overlap

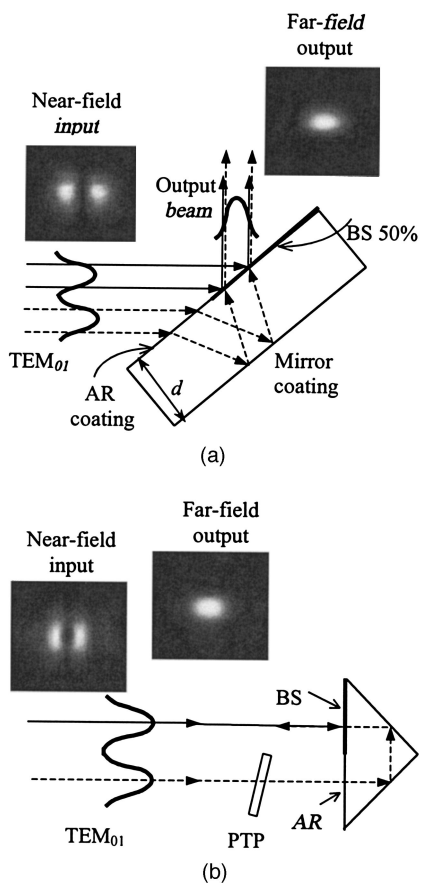


Fig. 2. Compact arrangements for obtaining a nearly Gaussian beam from a TEM_{01} mode: (a) compact single-plate mode converter; (b) compact-prism mode converter.

optimally at a 45° incident angle, the thickness d of the plate should obey

$$2d \tan\left(\arcsin \frac{1}{\sqrt{2n}}\right) = \sqrt{2}x_0, \quad (1)$$

where n is the refractive index of the plate material and x_0 is the required shift between the two lobes. The relative phase between the two lobes of the TEM_{01} distribution can be adjusted by a slight tilting of the plate, so their fields are combined coherently.

With the plate arrangement it is possible not to do the AR coating on one half of the plate. In this case the incident angle should be the Brewster's angle (55.4° for fused silica), and the incident TEM_{01} mode should be P polarized.

The arrangement for symmetrical folding of the lobes, shown in Fig. 1(b), can be made more compact by exploiting a special prism, as shown schematically in Fig. 2(b). The incident beam is a pure p -polarized TEM_{01} mode distribution. The crucial element is a high-precision 90° prism with specially designed coatings. Half of the prism front surface is coated with an AR coating, while the other half has a 50% BS coating. The sharp border between the two coatings is carefully aligned along the symmetry axis between the two lobes of the TEM_{01} -mode distribution. One

of the lobes is directly transmitted through the AR region, is totally reflected back, and exits the prism collinearly with the other reflected lobe field, and the two lobes are coherently combined on the 50% BS. A phase-tuning plate inserted in the path of one of the lobes field adjusts the relative phase between the lobes. In order to separate the incident field from the output field, the prism can be tilted slightly from the vertical orientation. Alternatively, the separation could be achieved with the aid of a PBS and a $\lambda/4$ plate before the prism, albeit with some losses due to polarization changes on reflections in the prism. Note that with this arrangement the field distribution of one lobe is not only shifted but also effectively flipped with respect to the other. Consequently the field distributions of the two lobes can completely coincide, so the power loss is negligible, as in the arrangement in Fig. 1(b). The beam-quality factor of the combined output beam should be $M_x^2 = 1.15$ and $M_y^2 = 1$, as for the one lobe of the TEM_{01} mode. The advantage of the single-prism converter compared with the single-plate converter is the possibility of exactly overlapping the distributions of the two lobes, including the tails, and the consequent absence of the ghost reflections from the AR-coated surface and other residual reflections.

Finally, all the above arrangements can also be used to convert a beam with a Gaussian distribution to that of a TEM_{01} distribution by simply reversing the direction of the beams.

3. Discussion

Since the two distributions of the individual lobes are combined coherently, it is best to have a maximal power P in one direction, so that the transformation efficiency will be maximal. The conversion efficiency can be written as

$$C = 1 - \frac{\int_{-\infty}^{\infty} |U_1(x) - U_2(x - x_0)|^2 dx}{2 \int_{-\infty}^{\infty} \{|U_1(x)|^2 + |U_2(x - x_0)|^2\} dx}, \quad (2)$$

where $U_1(x)$ and $U_2(x - x_0)$ are the field distributions of the two lobes of the TEM_{01} mode, which have the same phase. The field distribution $U_2(x - x_0)$ is effectively shifted by the shift parameter x_0 . Note that in the arrangements in Figs. 1(b) and 2(b) the distribution U_2 is not only shifted but first flipped with respect to U_1 (flipped in such a way that the initial distance between the peaks remains the same). Figure 3 shows the calculated conversion efficiency as a function of the relative shift parameter x_0/w , where w is the waist parameter of the TEM_{01} mode. Curve (a) shows the efficiency calculated for the nonsymmetrical folding arrangement shown in Fig. 1(a). Curve (b) shows the efficiency calculated for the symmetrical folding arrangement with flipped distribution U_2 , as shown in Fig. 1(b). As is evident, the maximal efficiency obtained for nonsymmetrical

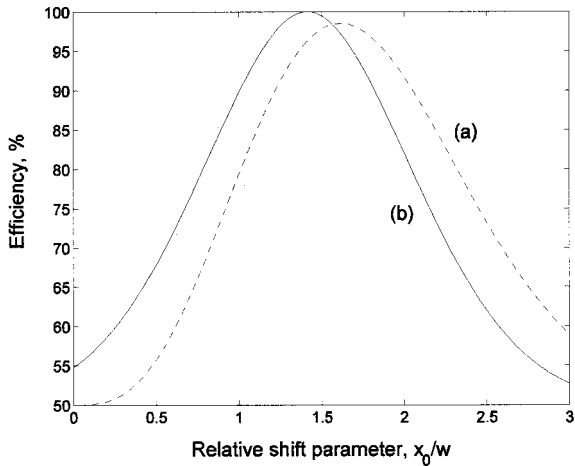


Fig. 3. Calculated conversion efficiency as function of the relative shift parameter x_0/w : (a), efficiency for the nonsymmetrical folding arrangements in Figs. 1(a) and 1(c); (b), efficiency for the symmetrical folding arrangement in Fig. 1(b). The maximal efficiency obtained for nonsymmetrical folding is 98.5% ($x_0/w = 1.62$), while for the symmetrical folding it is 100% ($x_0/w = 1.41$).

folding arrangements is 98.5% ($x_0/w = 1.62$), while for the symmetrical folding arrangement it is 100% ($x_0/w = 1.41$).

Now the beam-quality factor M^2 of the combined beam along the x direction¹¹ is

$$M_x^2 = 4\pi\sigma_x\sigma_{s_x}, \quad (3)$$

where σ_x and σ_{s_x} are the near-field and the far-field standard deviations of the beam-intensity profile in the x direction. (The spatial frequency s_x is related to the propagation angle θ by $s_x = \sin \theta/\lambda$.) Using Eq. (2), we calculated M_x^2 of the combined output beam as a function of the relative shift parameter x_0/w . The results are in Fig. 4. Curve (a) shows the beam-quality factor M_x^2 calculated for the non-

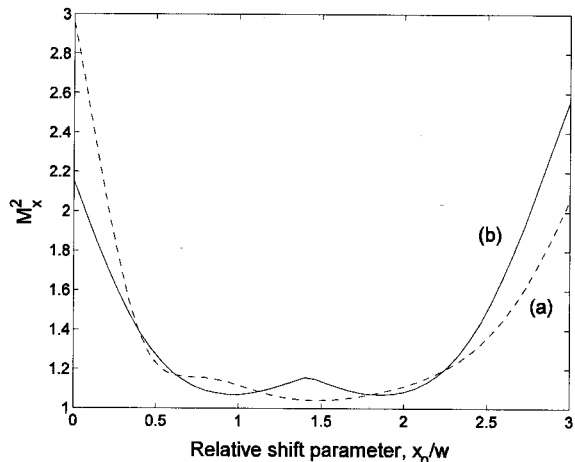


Fig. 4. Calculated beam-quality factor M_x^2 as a function of the relative shift parameter x_0/w : (a), nonsymmetrical folding arrangements in Figs. 1(a) and 1(c); (b), symmetrical folding arrangement in Fig. 1(b).

symmetrical folding arrangement in Fig. 1(a). Here $M_x^2 = 1.045$ at the optimal value of $x_0 = 1.62w$, being very close to the diffraction limit. Curve (b) shows the beam-quality factor M_x^2 calculated for the symmetrical folding arrangement of Fig. 1(b). Here $M_x^2 = 1.15$ at the optimal value of $x_0 = 1.41w$, as the M_x^2 value of a single TEM_{01} lobe. Note that the M_x^2 obtained for the optimal nonsymmetrical folding arrangement is smaller than that obtained for the optimal symmetrical folding arrangement. This is because the combined sum of the two lobe distributions is more symmetric and smooth for the nonsymmetrical folding arrangement; hence they resemble a Gaussian better than each lobe separately.

As is evident, there is a significant reduction in the M_x^2 value, from 3 for the TEM_{01} mode¹¹ to 1.045 or 1.15. Since the M_y^2 factor (in the y direction) remains 1, the effective cylindrical M^2 value¹² will be $M^2 = (M_x^2 + M_y^2)/2 = 1.0225$ for the nonsymmetrical folding arrangement and $M^2 = 1.075$ for the symmetrical folding arrangement, both comparable with that of an ideal Gaussian-beam distribution.

The calculated conversion efficiencies and the beam-quality factors for the compact arrangements in Fig. 2 are essentially the same. For the arrangement with the single plate in Fig. 2(a), some part of the tail in the transmitted lobe distribution is not reflected back and coherently summed at the output. Thus the power loss is reduced, but the output beam quality is somewhat deteriorated. The calculated conversion efficiency calculated for this arrangement has a maximum of 98.9% at a shift of $x_0 = 1.6w$, where the calculated M_x^2 value is 1.54.¹³ For the arrangement with the prism in Fig. 2(b) the folding is symmetrical and the results are the same as curves (b) in Figs. 3 and 4.

4. Experimental Procedure and Results

We experimentally evaluated the arrangements presented in Figs. 1(a), 2(a), and 2(b). The TEM_{01} mode distribution was derived from either a cw or a pulsed Nd:YAG laser in which a discontinuous phase element was inserted into the cavity.^{1,2}

The cw diode-pumped Nd:YAG laser was used with the conversion arrangement in Fig. 1(a). The laser configuration included a plano-convex ($R = 1.5$ -m) 60-cm-long resonator, an intracavity aperture of 1.6 mm, and a TEM_{01} mode selecting phase element. The laser was operated with output power of ~ 2 W. The corresponding pump power was close to the threshold of the laser. The measured focal length of the rod due to thermal lensing was ~ 70 cm.

The flashlamp-pumped pulsed Nd:YAG laser was used with the conversion arrangements in Fig. 2. The laser configuration included a plano-concave 70-cm-long resonator ($R = 3$ m), an intracavity aperture of 1.9 mm, and a TEM_{01} -mode-selecting phase element positioned ~ 9 cm from the rear mirror. The output beam was P polarized, and the pulse width was ~ 120 μ s. The laser operated not far from the threshold at a rate of 4 pps, and the output power was ~ 60 mW (15 mJ/pulse). For optimal overlap to be

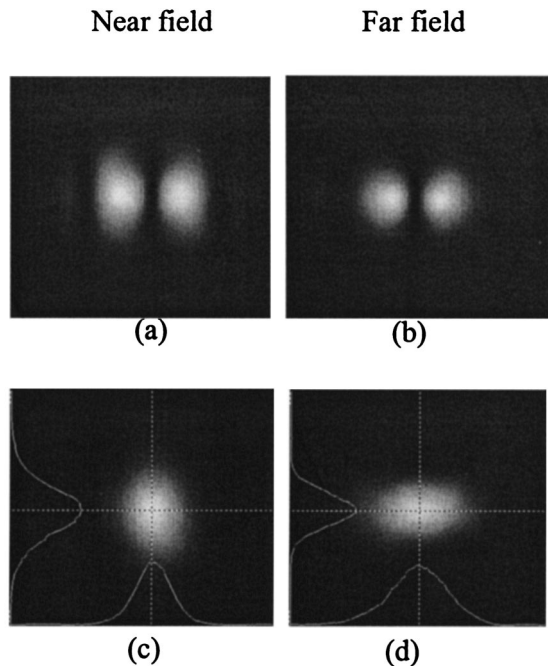


Fig. 5. Experimental results obtained with the arrangement in Fig. 1(a): (a), (b) near-field and far-field intensity distributions of the incident TEM_{01} beam derived from a cw Nd:YAG laser; (c), (d) near-field and far-field intensity distributions of the high-quality, nearly Gaussian output beam. The cross sections in x and y directions are shown at the bottom and left sides.

conveniently obtained between the two lobes of the TEM_{01} distribution with these arrangements, the beam from the laser was externally magnified with a variable zoom telescope so as to be compatible with the thickness of the mode-converting element and/or in order to collimate the beam. The plate in the arrangement shown in Fig. 2(a) had a thickness of 3 mm and parallelism of 1 arc sec, and appropriate dielectric coatings for P polarization and was aligned at an approximate angle of 45° relative to the incident beam. The angle was fine tuned so the field from the two lobes coherently adds up at the output. We found that the fine adjustment of the angle had an insignificant effect on the relative transverse shift between the lobe distributions. To reduce ghost reflections from the AR-coated surface and other residual reflections, we used a one-dimensional aperture with sharp edges so as to pass only the relevant light distributions. In the arrangement with the prism shown in Fig. 2(b) we used a prism whose angular deviation from 90° was less than 10 arc sec.

The experimental results are presented in Figs. 5–7. Figure 5 shows the experimental results obtained with the arrangement shown in Fig. 1(a), all detected with a CCD camera. Figures 5(a) and 5(b) show, respectively, the near-field and the far-field intensity distributions of the incident beam that was derived from the cw Nd:YAG laser. The far-field intensity distribution was obtained by focusing the beam with a spherical lens ($f = 101$ cm). These results indicate that the incident TEM_{01} distribution

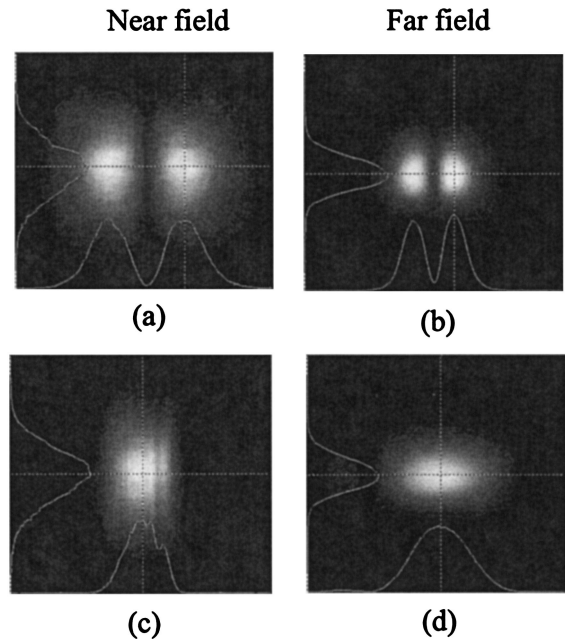


Fig. 6. Experimental results obtained with the arrangement in Fig. 2(a): (a), (b) near-field and far-field intensity distributions of the incident TEM_{01} beam derived from a pulsed Nd:YAG laser; (c), (d) near-field and far-field intensity distributions of the combined nearly Gaussian output beam.

is quite pure, with $M_x^2 = 3.21$ and $M_y^2 = 1.1$, which is slightly larger than the theoretical values $M_x^2 = 3$ and $M_y^2 = 1$. Thus it should be possible to transform the distribution into a high-quality nearly

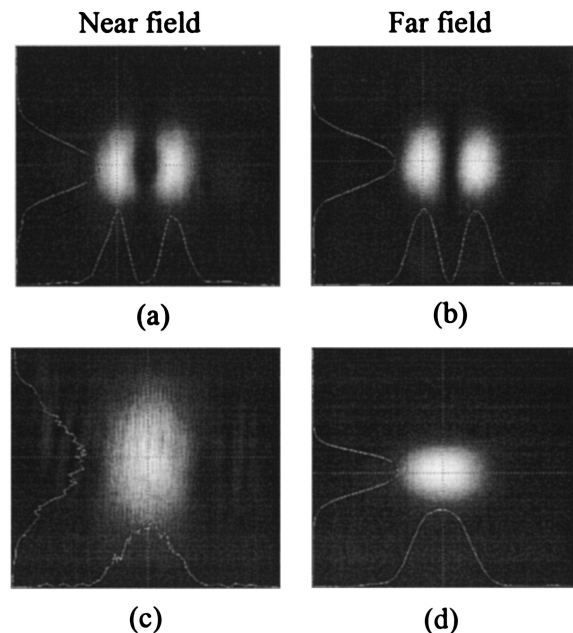


Fig. 7. Experimental results obtained with the arrangement in Fig. 2(b): (a), (b) near-field and far-field intensity distributions of the incident TEM_{01} beam derived from a pulsed Nd:YAG laser; (c), (d) near-field and far-field intensity distributions of the output nearly Gaussian beam.

Gaussian beam. The TEM₀₁ mode was then introduced into the arrangement shown in Fig. 1(a). The mirrors and beam splitter were carefully adjusted for optimal overlap of the lobe distributions, both in the near field and far field, and the phase tuning plate was rotated until complete constructive interference was obtained at the output.

This procedure ensured that the directions of the two beams were completely matched, and there is no phase difference between the beams. Note that the coherent summation should be made sufficiently close to the original beam waist in order to minimize the wavefront curvature of either beam. In our experiments the optical distance from the output coupler was ~35 cm, while the Rayleigh distance was ~3 m. The experimental near-field and far-field intensity distributions of the combined output beam are shown in Figs. 5(c) and 5(d), respectively. Both have the expected shape of one bright spot with nearly Gaussian cross sections in both the x and the y directions. Using these results, we calculated that $M_x^2 = 1.34$ for the output beam, somewhat higher than the expected value of 1.045. We attribute this discrepancy to a possible impurity in the incident beam. Yet there is reasonable agreement between the predicted and experimental results, proving the validity of our approach. We found that the experimental arrangement in Fig. 1(a) is rather sensitive to the mechanical and thermal vibrations and requires continuous control. Typically the optimal output distribution was stable for only 20–40 min.

Figure 6 shows the experimental results obtained with the arrangement in Fig. 2(a). Figures 6(a) and 6(b) show the near-field and the far-field intensity distributions of the incident TEM₀₁ beam that was derived from a pulsed Nd:YAG laser. The M^2 factor calculated for this beam¹² was 3.04 in the x direction and 1.16 in the y direction, indicating a nearly pure TEM₀₁ distribution. Figures 6(c) and 6(d) show, respectively, the near-field and the far-field intensity distributions of the combined output beam that emerges from the compact conversion arrangement. As is evident, both the near-field and the far-field intensity distributions have a single high-intensity lobe with nearly Gaussian profile cross sections in both axes.

Using these results, we calculated values of $M_x^2 = 1.21$ and $M_y^2 = 1.05$ for the output beam along with a total measured power efficiency of 91%, i.e., a 9% power loss. This indicates that the ratio of the power to $M_x^2 \times M_y^2$ (proportional to the brightness) is increased by a factor of 2.5 after the conversion and clearly demonstrates that M^2 of the output beam is closer to that of TEM₀₀. The 9% power loss can be attributed to the inexact overlap of the fields of the two-lobe distributions as well as the possible impurity of the original TEM₀₁ incident beam, pulse-to-pulse fluctuations of its intensity distribution and direction, and imperfect dielectric coatings. Even with this loss the results indicate a relatively efficient conversion to a nearly Gaussian beam. We found that the output distribution was much more stable

with the arrangement in Fig. 2(a) than that of Fig. 1(a). Indeed it remained stable during the entire experiment (several days).

Figure 7 shows the experimental results obtained with the arrangement shown in Fig. 2(b). Figures 7(a) and 7(b) show the experimental near-field and far-field intensity distributions of the incident TEM₀₁ beam derived from a pulsed Nd:YAG laser. The calculated M^2 for this beam was 3.09 in the x direction and 1.16 in the y direction, being very close to the theoretical values of 3 and 1. Figures 7(c) and 7(d) show the near-field and the far-field intensity distributions of the combined output beam that emerges from the mode converter. Both the near- and the far-field intensity distributions consist of a single high-intensity lobe with nearly Gaussian cross sections in both directions. Using these results, we calculated that $M_x^2 = 1.37$ and $M_y^2 = 1.39$ rather than the theoretical values of 1.15 and 1.

The separation between the input and the output beam was performed by introducing a polarizing beam splitter and a $\lambda/4$ plate before the prism. The power efficiency was measured by replacing the prism with a mirror of 99% reflectivity. The measured conversion efficiency was 93%, indicating a 7% power loss. This loss can be attributed to several factors: inexact overlap of the fields of the two-lobe distributions, possible impurity of the original TEM₀₁ input beam, pulse-to-pulse fluctuations of its intensity distribution and direction, imperfect dielectric coatings, and possible rotations of the polarization on the total internal reflections in the prism. Even with this loss these results indicate a relatively efficient conversion to a nearly Gaussian beam. We found that the stability of the output distribution with the arrangement in Fig. 2(b) was comparable with that of Fig. 2(a).

All the proposed conversion arrangements can also be used to convert a Gaussian-beam distribution to that of a TEM₀₁ distribution, simply reversing the direction of the beams. To illustrate this, we performed an experiment with the single-interferometric-element arrangement in Fig. 2(a). We used a Gaussian beam derived from an Nd:YAG laser and reversed the direction of propagation in the conversion arrangement. Specifically, the Gaussian beam was incident at the BS interface of the plate converter, and the output TEM₀₁ distribution emerged from the AR-coated and BS interfaces. The experimental results are shown in Fig. 8. Figures 8(a) and 8(b) show the near-field and the far-field intensity distributions of the incident Gaussian beam. Figure 8(c) shows the near-field intensity distribution of the output TEM₀₁ distribution. Figure 8(d) shows the far-field intensity distribution of the output TEM₀₁ beam distribution, when the two near-field lobes have the same phase. As expected, there is a bright central lobe with two low-intensity side-lobes. Figure 8(e) shows the far-field intensity distribution of the output TEM₀₁ beam distribution, when the two near-field lobes have a π phase shift (a

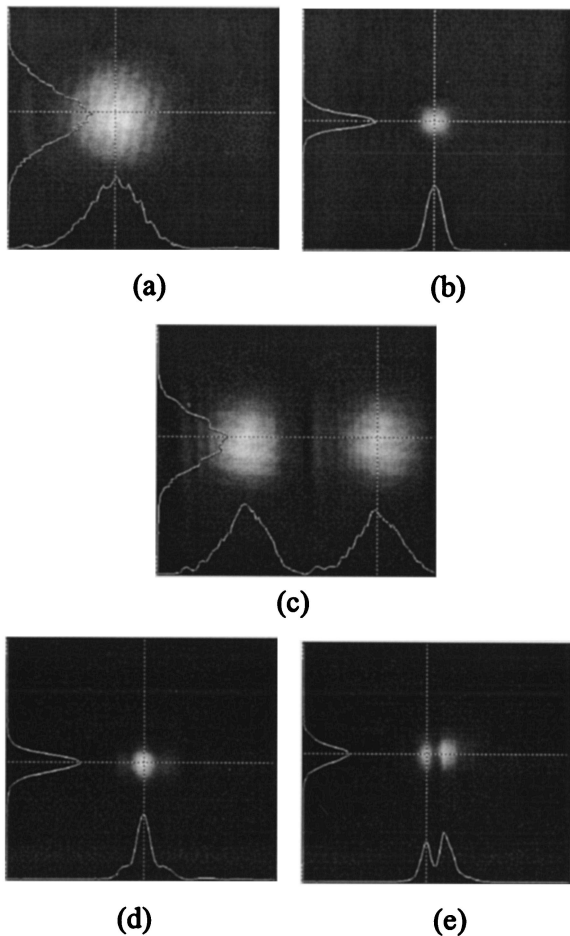


Fig. 8. Conversion of a Gaussian distribution into a TEM_{01} mode distribution by using the single-interferometric-element arrangement in Fig. 2(a): (a), (b) near-field and far-field intensity distributions of the incident Gaussian beam; (c) near-field intensity distribution of the TEM_{01} output beam; (d) far-field intensity distribution of the TEM_{01} output beam when the phase of each lobe in the near field is the same; (e) far-field intensity distribution of the TEM_{01} output beam with a conventional TEM_{01} phase distribution.

real TEM_{01} mode distribution). The phase-shift control is achieved by carefully tilting the plate.

5. Concluding Remarks

We have presented several optical arrangements for efficiently converting a high-order TEM_{01} distribution into a nearly Gaussian-beam distribution, thereby improving beam quality. These arrangements have included several discrete optical elements and some more compact and robust arrangements with a single specially coated interferometric element. Several conversion arrangements have been experimentally evaluated, and the experimental results were close to those predicted, with conversion efficiencies greater than 90%. It is

possible to extend the arrangements to allow conversion of higher-order-mode distributions to a Gaussian distribution. For example, the TEM_{02} mode distribution, which is composed of four identical nearly Gaussian lobes and having $M_x^2 = M_y^2 = 3$,¹² can be converted to a single Gaussian distribution by resorting to double and folded arrangements in the two perpendicular directions.

Finally, we can also exploit all the arrangements to convert a single Gaussian distribution into a high-order mode distribution by simply reversing the direction of the light propagation in the conversion arrangements.

This research was supported in part by Parnot Venture Capital Fund through Impala, Ltd.

References

1. R. Oron, N. Davidson, A. A. Friesem, and E. Hasman, "Transverse mode shaping and selection in laser resonators," *Prog. Opt.* **42**, 325–385 (2001).
2. A. A. Ishaaya, N. Davidson, G. Machavariani, E. Hasman, and A. Friesem, "Efficient selection of high-order Laguerre–Gaussian modes in a Q-switched Nd:YAG laser," *J. Quantum Electron.* **39**, 74–82 (2003).
3. A. A. Napartovich, N. N. Elkin, V. N. Troschieva, D. V. Vyotsky, and J. R. Leger, "Simplified intracavity phase plates for increasing laser-mode discrimination," *Appl. Opt.* **38**, 3025–3029 (1999).
4. M. Gerber and T. Graf, "Generation of super-Gaussian modes in Nd:YAG lasers with graded-phase mirrors," in *Proceedings of International Conference on Advanced Laser Technologies*, 15–20 September 2002, Adelboden, Switzerland, pp. 3–4.
5. T. Graf and J. E. Balmer, "Laser beam quality, entropy and the limits of beam shaping," *Opt. Commun.* **131**, 77–83 (1996).
6. P. W. Rhodes and D. L. Shealy, "Refractive optical systems for irradiance redistribution of collimated radiation: their design and analysis," *Appl. Opt.* **20**, 3545–3553 (1980).
7. O. Bryngdahl, "Geometrical transformations in optics," *J. Opt. Soc. Am.* **64**, 1092–1099 (1974).
8. M. T. Eismann, A. M. Tai, and J. N. Cederquist, "Iterative design of a holographic beamformer," *Appl. Opt.* **28**, 2641–2650 (1989).
9. N. Davidson, A. A. Friesem, and E. Hasman, "Diffractive elements for annular laser beam transformation," *Appl. Phys. Lett.* **61**, 381–383 (1992).
10. G. Machavariani, N. Davidson, A. A. Ishaaya, A. A. Friesem, and E. Hasman, "Efficient formation of a high-quality beam from a pure high-order Hermite–Gaussian mode," *Opt. Lett.* **27**, 1501–1503 (2002).
11. A. E. Siegman, "New developments in laser resonators," in *Optical Resonators*, D. A. Holmes, ed., *Proc. SPIE* **1224**, 2–14 (1990).
12. J. B. Murphy, "Phase space conservation and selection rules for astigmatic mode converters," *Opt. Commun.* **165**, 11–18 (1999).
13. A. A. Ishaaya, G. Machavariani, N. Davidson, A. A. Friesem, and E. Hasman, "Conversion of a high-order mode beam into a nearly Gaussian beam using a single interferometric element," *Opt. Lett.* **28**, 504–506 (2003).